

May 19, 1999

# Simulation of Photomultiplier Response

I. Fedorko, S. Tokar,

Dept. of Nuclear Physics, Comenius University, Mlynská dolina F1,  
SK-84215 Bratislava, Slovakia

I. Chirikov-Zorin

Joint Institute for Nuclear Research, 141980 Dubna, Moscow Region, Russia.

## Abstract

A code for simulation of photomultiplier response was created and tested for a broad range of photomultiplier gain. A reasonably good agreement between the experimental R5900 spectra and simulated ones was achieved. It was shown that for correct explanation of the charge fluctuations in the observed R5900 single photoelectron spectra the dynode inhomogeneity and first dynode effect should be taken into account. The value of the inhomogeneity was estimated to be about 25%.

## 1 Introduction

Good understanding of photomultiplier (PMT) response in the case when a few photoelectrons are created on photocathode (faint input light signals) is of a principal value for finding out the global properties of the PMT based spectrometric systems. So called single photoelectron analysis can be used for determining of some important PMT characteristics, which can be used for finding out such calorimeter parameters like the energy conversion factor (GeV-to-photoelectrons), etc. In this work we simulated the PMT responses in different regimes of the PMT with the metal channel dynode system structure mainly for the purpose of single photoelectron analysis. The main goal was to optimize the PMT response function needed for the single photoelectron analysis of the metal channel PMTs like Hamamatsu R5900 [1], [2].

## 2 Simulation of photomultiplier response

The core of PMT response simulation consists in simulation of electron cascade multiplication process that occur in dynode system of PMT. This process essentially obeys Poisson law but, nonetheless, for correct understanding of the



PMT response the different physical phenomena (inhomogeneities, photoelectric effect on the first dynode, etc.) in the PMT should be taken into account. The correct PMT response function must reflect the PMT structure from the view point of light conversion and charge multiplication. The operating principles and construction of the PMT have in general four essential elements : a *photocathode*, an *electron-optical system*, an *electron multiplier* and an *anode*, which collects the electron flux. For our purpose the PMT processes can be divided in two independent parts :

- photoconversion and subsequent photoelectron collection,
- amplifications in dynode system and collection on anode.

## 2.1 Photoconversion

We assume to have a pulsed source of light with the constant amplitude. A certain portion of the emitted photons are hitting the PMT photocathode - this number is a Poisson random variable [3]. The incident photons (picked up by photocathode) can produce photoelectrons via photoelectric effect. The conversion of photons into electrons and their subsequent collection is a random binary process. Therefore the distribution of the number of photoelectron collected from photocathode is a convolution of Poisson and binary processes which again gives a Poisson distribution:

$$P_\mu(n) = \frac{\mu^n e^{-\mu}}{n!}, \quad (1)$$

where  $\mu$  is the mean number of photoelectrons captured by dynode system and  $P_\mu(n)$  is the probability that  $n$  photoelectrons will be captured when their mean is  $\mu$ . It is important to note that  $\mu$ , defined as

$$\mu = m \cdot \eta \quad (2)$$

where  $\eta$  is the photocathode quantum efficiency and  $m$  is the mean number of photons hitting photocathode, characterizes not only light source intensity but also quantum efficiency.

## 2.2 Charge multiplication

Dynode system multiplies input photoelectron signal via the effect of secondary emission. In our model the number of secondary electrons is assumed to obey Poisson law. Secondary emission coefficient is a function of incident electron energy [4],[5]. In electron multiplier, the energy of the electrons incident on each stage is a function of the potential difference between the dynodes. We assume 100% efficiency of electrons collection on dynodes, then the emission coefficient  $k_i$  is

$$k_i = \text{const} \cdot (U_i)^\kappa \quad (3)$$

where  $U_i$  is voltage between  $(i-1)^{th}$  and  $i^{th}$  dynode,  $\kappa$  is an exponent varying from 0.5 to 0.9, and *const* is inferred from gain.

$$G = \prod_{i=1}^N k_i \quad (4)$$

where  $N$  is the total number of stages. As can be seen from the above mentioned, the mean value of the secondary emission coefficient is a function of gain, repartition ratio and exponent  $\kappa$

$$k_i = \left( \frac{G}{\left( \prod_{i=1}^N r_i \right)^\kappa} \right)^{\frac{1}{N}} \cdot (r_i)^\kappa \quad (5)$$

where the repartition ratio  $r_1 : r_2 : \dots r_N$  is the same like the ratio of the applied voltages  $U_1 : U_2 : \dots U_N$ . Using this equation we can find the secondary emission coefficient for each dynode.

### 2.3 Additional processes

In a realistic PMT there are some additional phenomena, which contributes to or influences the output signal. In the presented model we have assumed four important sources of fluctuations:

- photoconversion of incident photons on the first dynode,
- collection of the photoelectron from photocathode by the second dynode,
- inhomogeneity of dynode system,
- photocathode inhomogeneity.

Photoconversion on the first dynode, if compared with that on photocathode, will lead to a lower output charge because charge multiplication starts only from the second dynode:

$$Q_2 = \frac{Q_1}{k_1} \quad (6)$$

Where  $Q_1$  ( $Q_2$ ) is the mean charge initiated by one photoelectron from photocathode (first dynode) and  $k_1$  is the secondary emission coefficient on the first dynode. In the case of a photoelectron emitted from the photocathode and collected on the second dynode, the charge multiplication also starts from the second dynode but in this case the secondary emission coefficient is enhanced due to higher acceleration voltage ( $U_1 + U_2$ ). In this case for the emission coefficient one can write:

$$k_2 = const \cdot \left( U_1 + U_2 \right)^\kappa \quad (7)$$

The inhomogeneity of dynode system means that the coefficient of secondary emission depends not only on energy of incident electron but also on the place of its incidence. This inhomogeneity, which plays an important role especially in the case of first dynode, will enhance the output charge fluctuations. The photocathode inhomogeneity, i.e. the dependence of quantum efficiency on the photon incidence place can also lead to an increase in the output charge fluctuations.

In some cases the output of dynode system, when the process is initiated by a big number of photoelectrons ( $n > 4$ ), can be approximated by a Gaussian distribution [1], [3].

A possibility to approximate by a Gaussian function the PMT model response initiated by a given number of photoelectrons is investigated provided that the PMT gain varies from  $10^4$  to  $10^7$ . It has been expected that the Gaussian approximation of the model response should be appropriate for three and more photoelectrons.

## 2.4 Simulation process

At the beginning of event we generate the number of hitting photons using Poisson law (1). Each photon has probability  $\eta$  to be converted in photoelectron. As a result a certain number of photoelectrons is created on the photocathode. These photoelectrons entering into the dynode system initiate a process of charge multiplication. For each photoelectron the number of secondary electrons created on the first dynode is generated using Poisson law - resulting in the first generation of secondary electrons. In an analogous way (using the same law) treating the first generation electrons one after another, the next (second) generation of electrons is produced. It should be noted that when the number of electrons in the current generation is bigger than a critical value (for the presented results  $\sim 50$ ), then the next generation of electrons is produced not by an individual treating of the current generation electrons but using a Gaussian distribution with the mean value  $Q$

$$Q = q \cdot k_i, \quad (8)$$

where  $q$  is the number of the incident electrons and  $k_i$  is the emission coefficient on the  $i^{\text{th}}$  dynode.

The additional processes are also taken into account in our model. The response due to the photoconversion on  $1^{\text{st}}$  dynode one can interpret as an additional charge, generated as well as normal case. For the electrons collected on the  $2^{\text{nd}}$  dynode the emission coefficient is given by (7). The inhomogeneity of dynode surfaces can be taken into account via randomizing of the secondary emission coefficient  $k_i$  values employing Gaussian distribution.

## 3 Results

In the first phase we simulated an 8-stage PMT with the gain varying from  $10^4$  to  $10^7$  assuming that the charge multiplication process is an ideal one, i.e. production of secondaries obeys Poisson law, no inhomogeneities are present, photoelectrons are created only on photocathode and collection efficiency of photoelectrons by dynodes system is 100%. In the simulation we have assumed that the intensity of input light is characterized in the mean by approximately two photoelectrons.

The results of this simulation are presented in Figs. 1-4, where the ideal case charge distributions initiated by  $n$  ( $=0, 1, 2, 3, 4$ , and  $6$ ) photoelectrons are shown for the gains  $10^4$ ,  $10^5$ ,  $10^6$  and  $10^7$ . We can conclude from these figures that at the high gains ( $>10^6$ ) the PMT response is symmetric (Gaussian) if the charge distribution is initiated by 3 or more photoelectrons. In other cases ( $n \leq 2$ ) the response is asymmetric. At low gains ( $<10^6$ ) the asymmetry is noticeable also in

the case of 3 photoelectrons. In Fig. 5 are presented the overall simulated ideal responses for the gains  $10^4$ ,  $10^5$ ,  $10^6$  and  $10^7$  assuming two photoelectrons light source intensity. The issues on the individual  $n$ -photoelectrons components of the simulated pulse height spectra are important for correct understanding of the single photoelectron analysis of the real PMT spectra, particularly for finding of the PMT noise factor and adjacent issues [6], [1], [7].

In Fig. 6 the experimental spectrum taken by the photomultiplier Hamamatsu R5900 (7M02C1) is shown. The applied voltage used in the measurement was  $925V$  with the voltage repartition  $2:2:1:1:1:2:3$ . The spectrum was deconvoluted by the method presented in [1]. The results of the deconvolution were used as the input data for simulation. To the input data taken from deconvolution of experimental case and subsequently used in simulation belong: the position and width of pedestal, the number of photoelectrons emitted from photocathode and the number of electrons contributed to the photoemission from first dynode and/or the number of photoelectrons from photocathode captured by second dynode.

The spectrum measured at  $925V$  and the simulated ideal one are compared in Fig. 7. The mean value of the total number of photoelectron generated on photocathode ( $a_{Phe} = 2.357$ ) was used as an input parameter for the ideal case simulation. One can see from this figure that the ideal case without other physical phenomena (green line in Fig 7) does not describe properly the real response, particularly a lack of events between the pedestal and one photoelectron peak is noticeable. We tried to cope with this event deficiency by including some additional processes into our model. We have included the effect of photoelectron production on first dynode and the effect of collection of photoelectrons (from photocathode) by second dynode. Both phenomena generate events behind the pedestal and form so called the first dynode effect. The magnitude of the effect is characterized by value of the parameter  $a_{Phe1}$  (for the spectrum in question  $a_{Phe1} = 0.235$ ) giving the number of photoelectrons created on first dynode or photoelectrons from photocathode captured by second dynode, at the same time the percentage of both processes can vary in a complementary way from 0% to 100%. Inclusion of the above mentioned processes helped to cure the event deficiency behind the pedestal, but was insufficient for a general agreement between the experimental spectrum and the simulated one. To find such an agreement we have added into the model also the inhomogeneity of dynode system, i.e. we let the coefficient of secondary emission to depend on the place of electron incidence (on given dynode). In case of the simulated spectrum the inhomogeneity has been treated only on the first two dynodes. The inhomogeneity effect on other dynodes has been ignored as the contributions of these dynodes to the output charge fluctuations are suppressed [6]. The photoelectrons contributing to the first dynode effect, given by parameter  $a_{Phe1}$ , have been divided according the ratio  $8:2$  between the photoproduction on the first dynode and collection of photoelectrons by the second one. As one can see from Fig. 7 inclusion of the above mentioned phenomena leads to a very good agreement between the experimental spectrum (solid black line) and the simulated one (solid red line). The best result in this case was found for the inhomogeneity of 25%. We started comparison between the experimental and simulated spectra at high gains ( $925V$ ) because the additional phenomena included in simulation should be more profound in the case of high gains (high voltages).

To compare experimental and simulated spectra in a broad range of gains we have simulated the more realistic cases, from the ATLAS point of view, which correspond to the real spectra taken at the voltages  $700\text{ V}$ ,  $750\text{ V}$ ,  $800\text{ V}$ , and  $850\text{ V}$ . The input parameters of the simulated spectra are in table 1.

Table 1: The input parameters for the simulated responses compared with the real spectra taken at voltage  $700\text{ V}$ ,  $750\text{ V}$ ,  $800\text{ V}$ , and  $850\text{ V}$ ,  $\delta$  is the dynode inhomogeneity.

voltage	700V	750V	800V	850V
$Q_{Ped}$	70.8	70.07	70.8	71.8
$\sigma_{Ped}$	1.6	1.8	1.8	1.8
$a_{Phe}$	2.	2.096	2.092	2.1
$a_{Phe1}$	0.22	0.292	0.3	0.34
events	129677	299240	407661	657323
gain	402446	660893	1045978	$1.595 \cdot 10^6$
$\delta$	25%	25%	25%	25%

Using the inhomogeneity of dynodes, the first dynode photoelectric effect and the direct capture of photoelectrons from photocathode on the second dynode we have looked for the best agreement between the experiment and simulation. From the same reason as before, in the results presented below, the dynode inhomogeneity was considered only on the first two dynodes. In the Fig. 8 is compared the real spectrum taken at ( $700\text{ V}$ ) with the simulated ideal one and the simulated one with all the mentioned processes involved. The optimal ratio of the first dynode photoelectric effect to the capture by the second dynode ( $r_{1D}$ ) was found to be  $5:5$ . For the spectra at voltages  $750\text{ V}$  (Fig. 9),  $800\text{ V}$  ( Fig. 10 ), and  $850\text{ V}$  ( Fig. 11) the optimal ratio was  $r_{1D} = 3:7, 4:6, 5:5$ , respectively. In all cases the dynode inhomogeneity was assumed to be 25%.

Essentially we can say that the agreement between the real and simulated spectra is good, if additional processes are taken into account. The fact that the value of the ratio  $r_{1D}$  is varying a little can be explained by the systematics of the method. The first dynode peak events is not easy to distinguish from those of the pedestal and also from the low tail one photoelectron events.

## 4 Conclusion

We built the model of photomultiplier's response which except of the standard processes occurring in photomultiplier as photoelectric effect on photocathode and charge multiplication in dynode system using Poisson law, takes into account also:

- photoconversion of incident photons on first dynode,
- collection of photoelectrons from photocathode on second dynode,
- inhomogeneity of PMT dynode system.

A good agreement between the experimental spectra and the simulated ones was achieved for a broad range of gains ( $10^5 - 10^7$ ).

From analysis of the simulated spectra at different gains it follows that the PMT response initiated by  $n$  photoelectrons at gains  $<10^6$  can be approximated by a Gaussian in cases, when more than 3 photoelectrons are emitted from photocathode and collected by dynode system. For the gains  $>10^6$  the Gaussian approximation is applicable for the responses initiated by 3 and more photoelectrons. If 1 or 2 photoelectrons are emitted, the PMT response should be expanded using Poisson distribution ( [1], [2] ). This fact is important for the single photoelectron spectra analysis of the metal dynode photomultiplier.

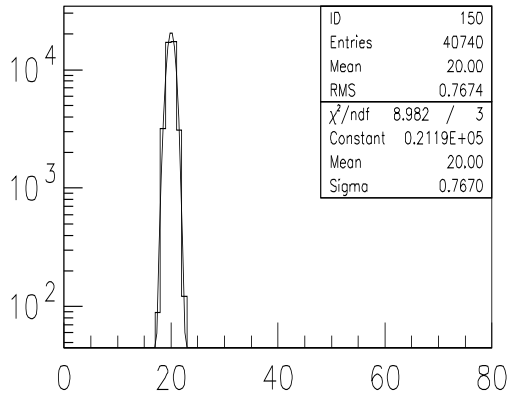
The photoelectric effect on first dynode and capture of photoelectrons from photocathode by second dynode can interpret an enhancement of events experimentally observed on the right tail of pedestal ( observed as a peak at high gains).

The inhomogeneity of the PMT dynode system must be taken into account for a correct explanation of the fluctuations present in the PMT output charge. The multiplication process using Poisson law for production of secondaries in dynode system underestimates these fluctuations and cannot be used for finding of the PMT noise factor needed for finding the energy conversion factor (GeV-to-photoelectron factor). For tested PMT Hamamatsu R5900 (7M02C1) the inhomogeneity was found to be 25%.

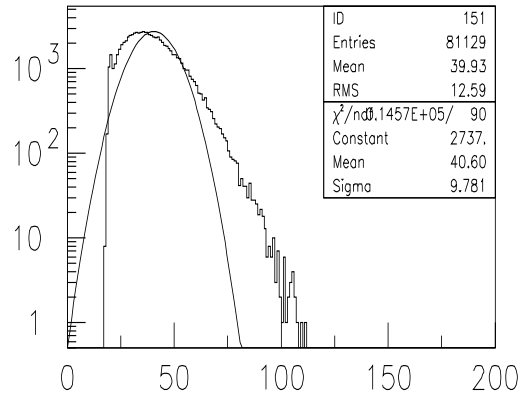
## References

- [1] S. Tokár, et al. Single photoelectron spectra analysis for the metal dynode photomultiplier. *ATLAS Internal Note*, ATL-TILECAL-99-005, 1999.
- [2] S. Tokar, et al. Single photoelectron spectra analysis for the metal dynode photomultiplier. *Acta Phys. Univ. Comeniana, Vo. 40 (1999) p.114*.
- [3] E.H.Bellamy, et al. Absolute calibration and monitoring of spectrometric channel using a photomultiplier. *Nucl. Instrum. Meth.A*, 339:486–476, 1994.
- [4] Philips catalog. *Photomultipliers tube, principles and applications*.
- [5] G.Barbiellini, et al. A simulation study of the behavior of fine mesh photomultipliers in magnetic field. *Nucl. Instrum. Meth.A*, 362:245–252, 1995.
- [6] G. Montarou, Ph. Grenier, et al. Characterization of the Hamamatsu 10-stages R5900 photomultipliers at Clermot for the tile calorimeter. *ATLAS Internal Note*, ATL-TILECAL-97-108, 1997.
- [7] S. Nemecek, et al. Light Yield Measurement of the 1998 Tile Barrel Module0 using muon beams. *ATLAS Internal Note*, ATL-TILECAL-99-003, 1999.

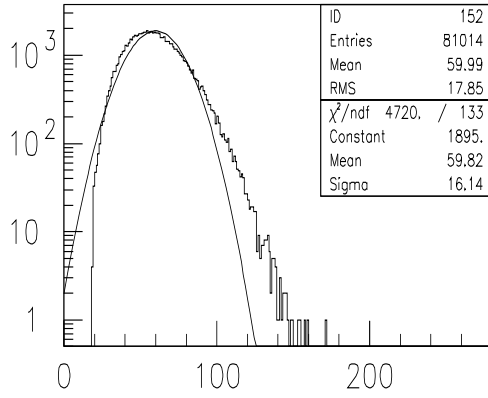




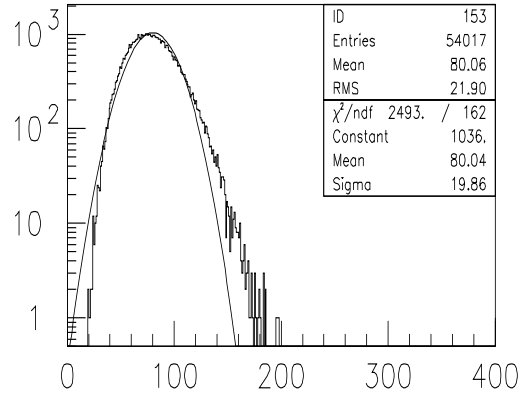
charge per 0 ph.e



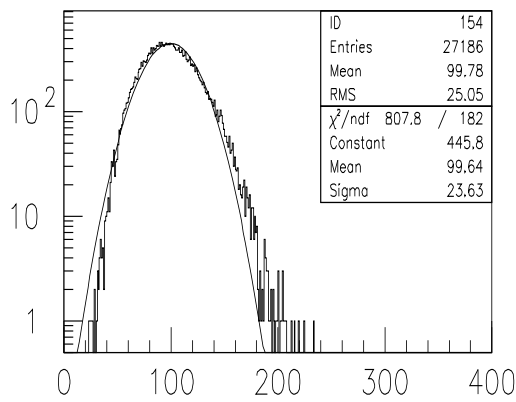
charge per 1 ph.e



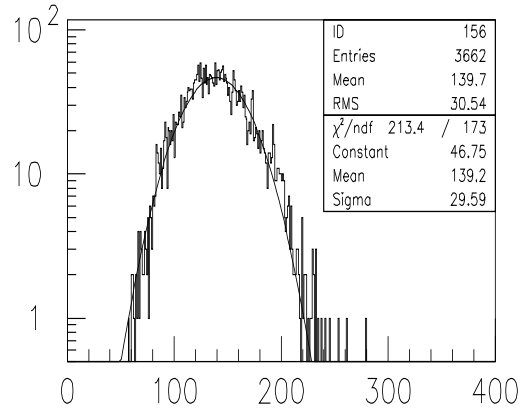
charge per 2 ph.e



charge per 3 ph.e

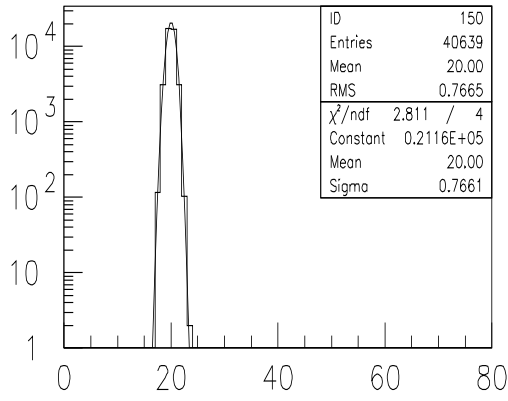


charge per 4 ph.e

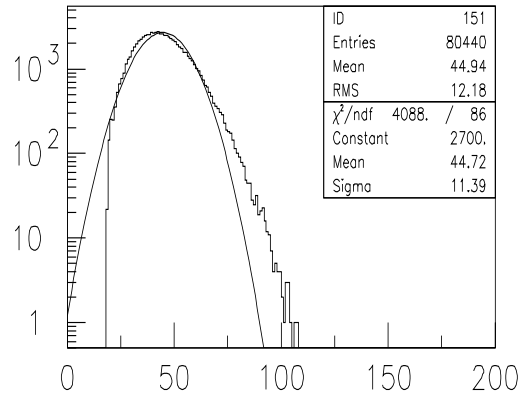


charge per 6 ph.e

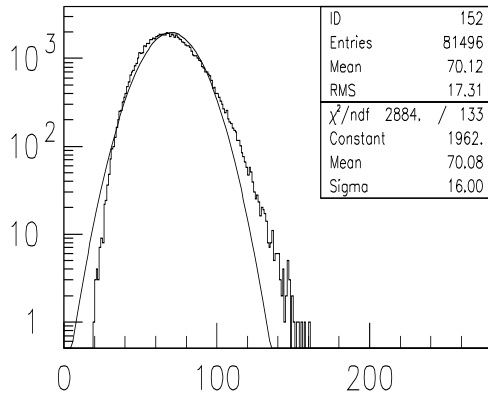
Figure 1: The output PMT charge distributions initiated by different number of photoelectrons (0,1,2,3,4 and 6) at the PMT gain  $10^4$ .



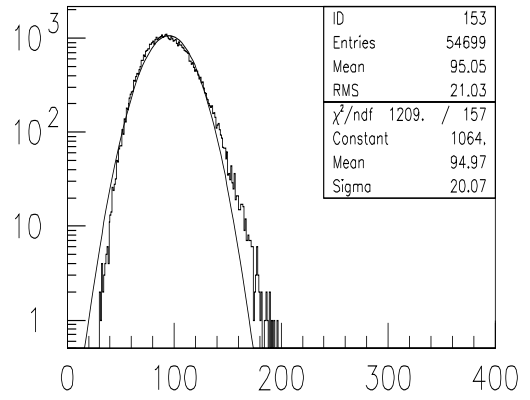
charge per 0 ph.e



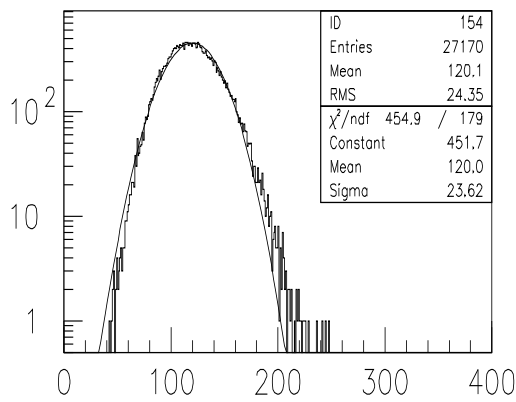
charge per 1 ph.e



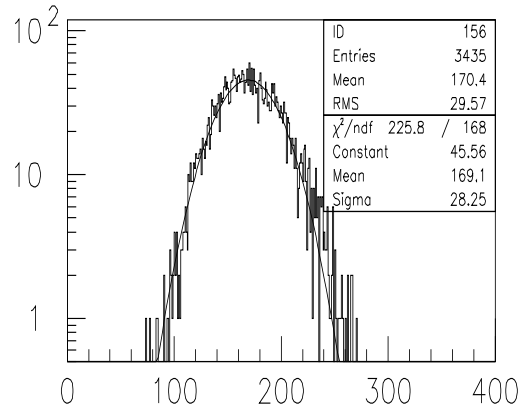
charge per 2 ph.e



charge per 3 ph.e

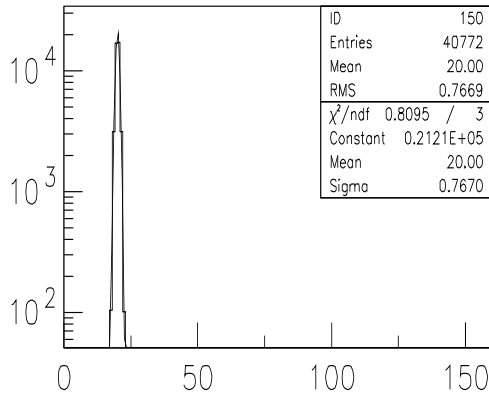


charge per 4 ph.e

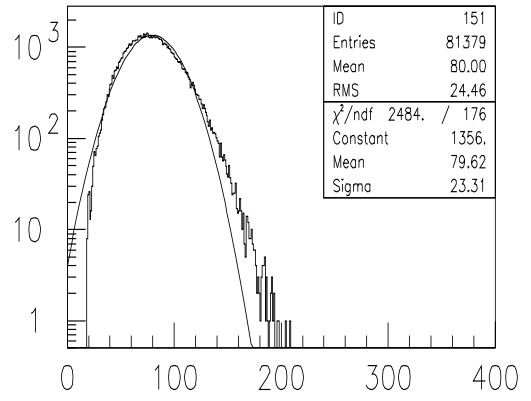


charge per 6 ph.e

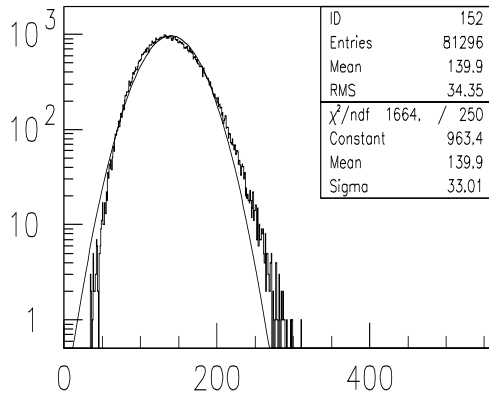
Figure 2: the PMT output charge distributions initiated by different number of photoelectrons (0,1,2,3,4 and 6) at the PMT gain  $10^5$ .



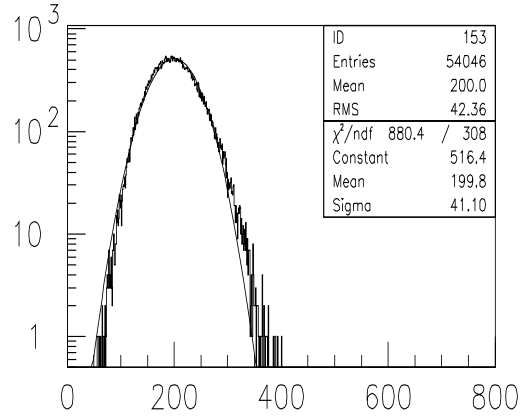
charge per 0 ph.e



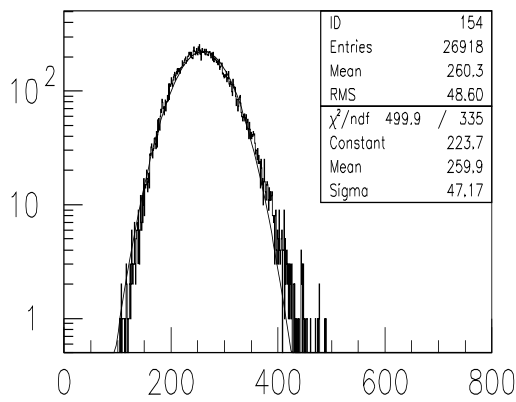
charge per 1 ph.e



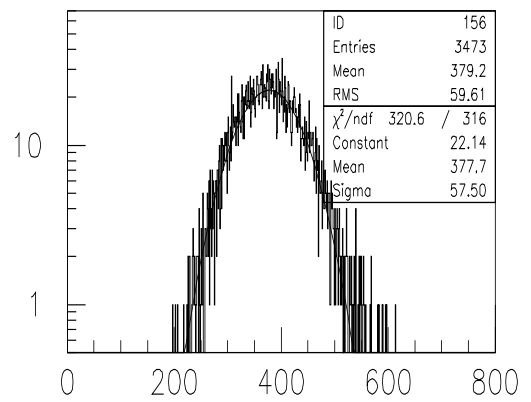
charge per 2 ph.e



charge per 3 ph.e

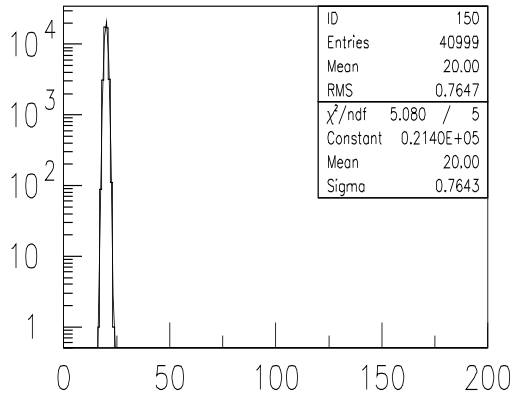


charge per 4 ph.e

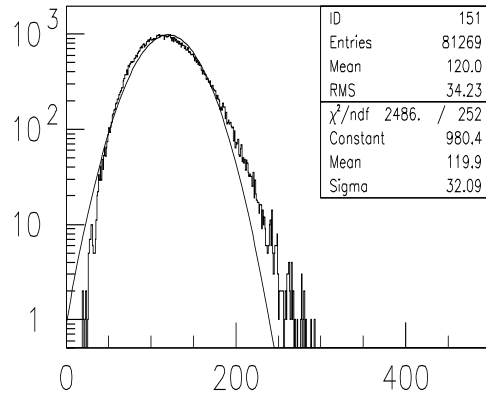


charge per 6 ph.e

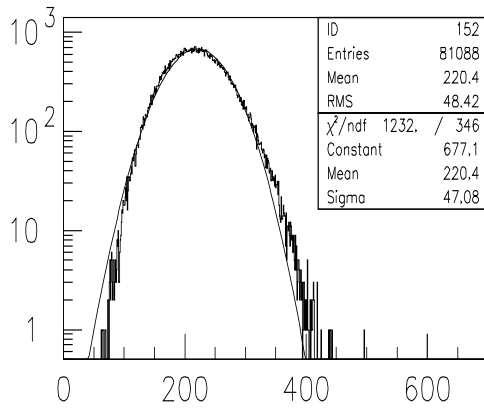
Figure 3: the PMT output charge distributions initiated by different number of photoelectrons (0,1,2,3,4 and 6) at the PMT gain  $10^6$ .



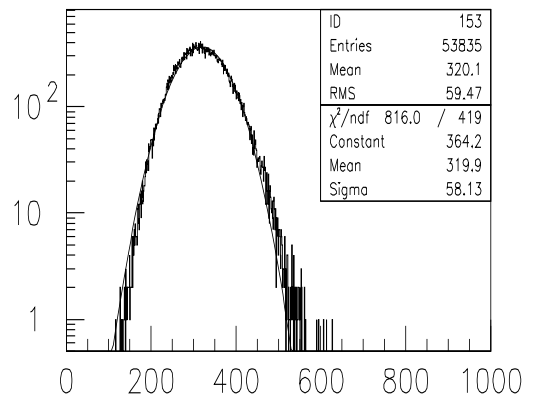
charge per 0 ph.e



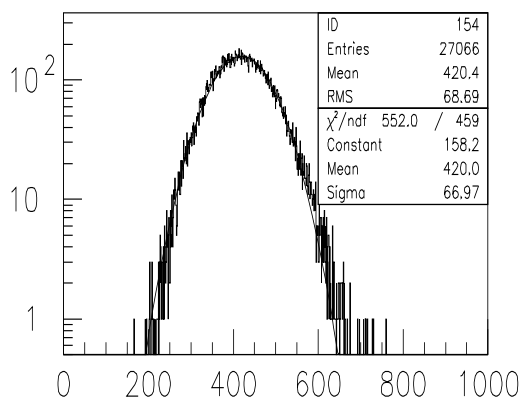
charge per 1 ph.e



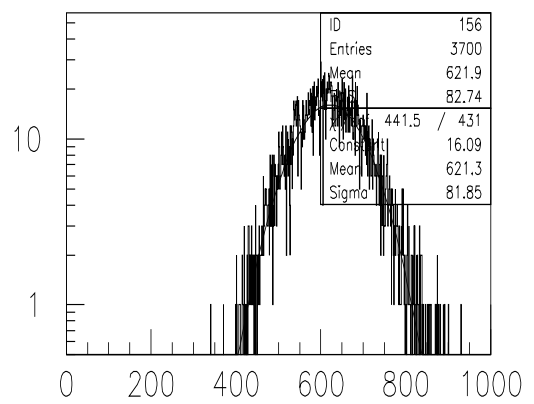
charge per 2 ph.e



charge per 3 ph.e



charge per 4 ph.e



charge per 6 ph.e

Figure 4: the PMT output charge distributions initiated by different number of photoelectrons (0,1,2,3,4 and 6) at the PMT gain  $10^7$ .

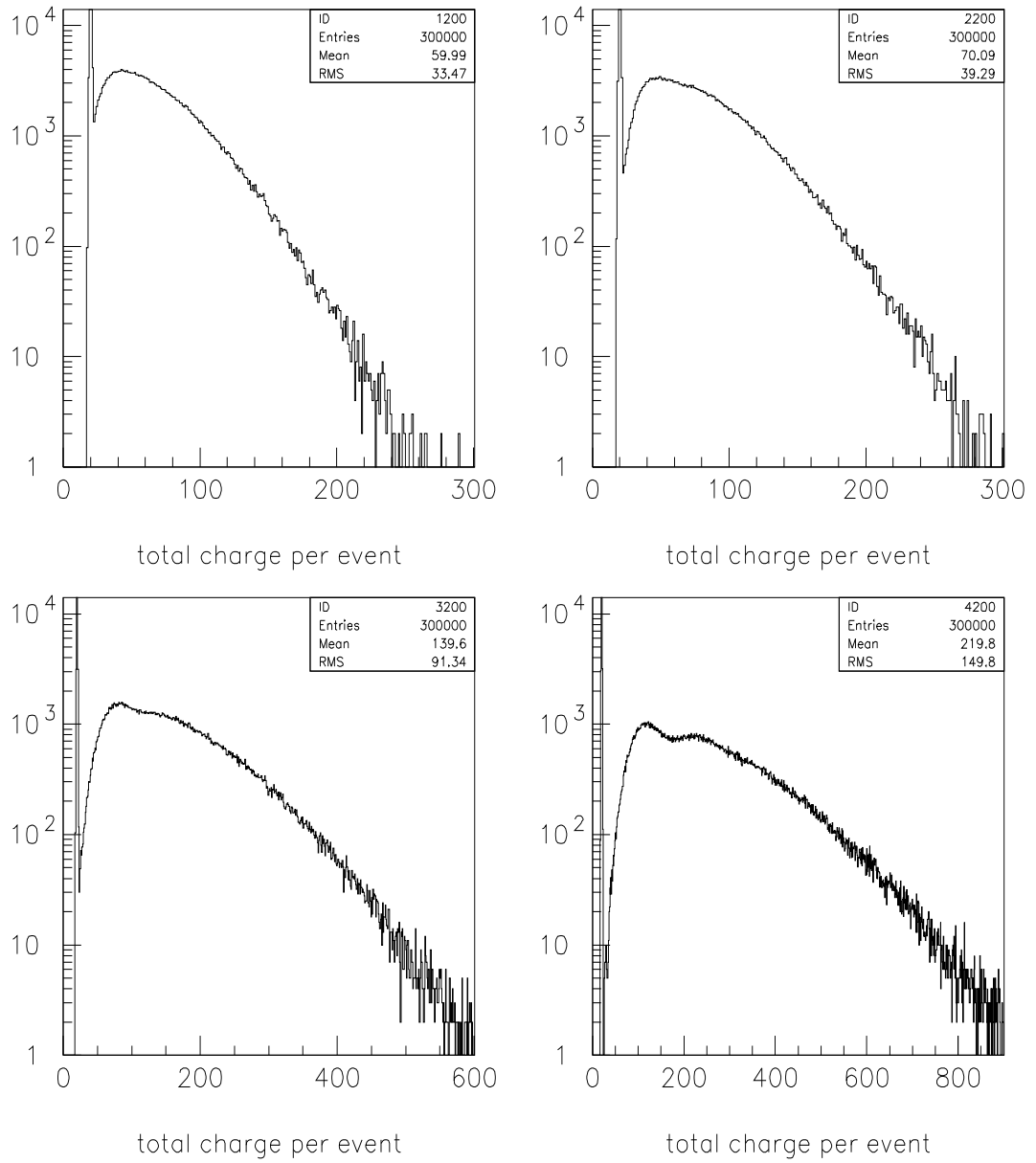


Figure 5: The simulated ideal responses for the gain values  $10^4$ ,  $10^5$ ,  $10^6$  and  $10^7$ , respectively.

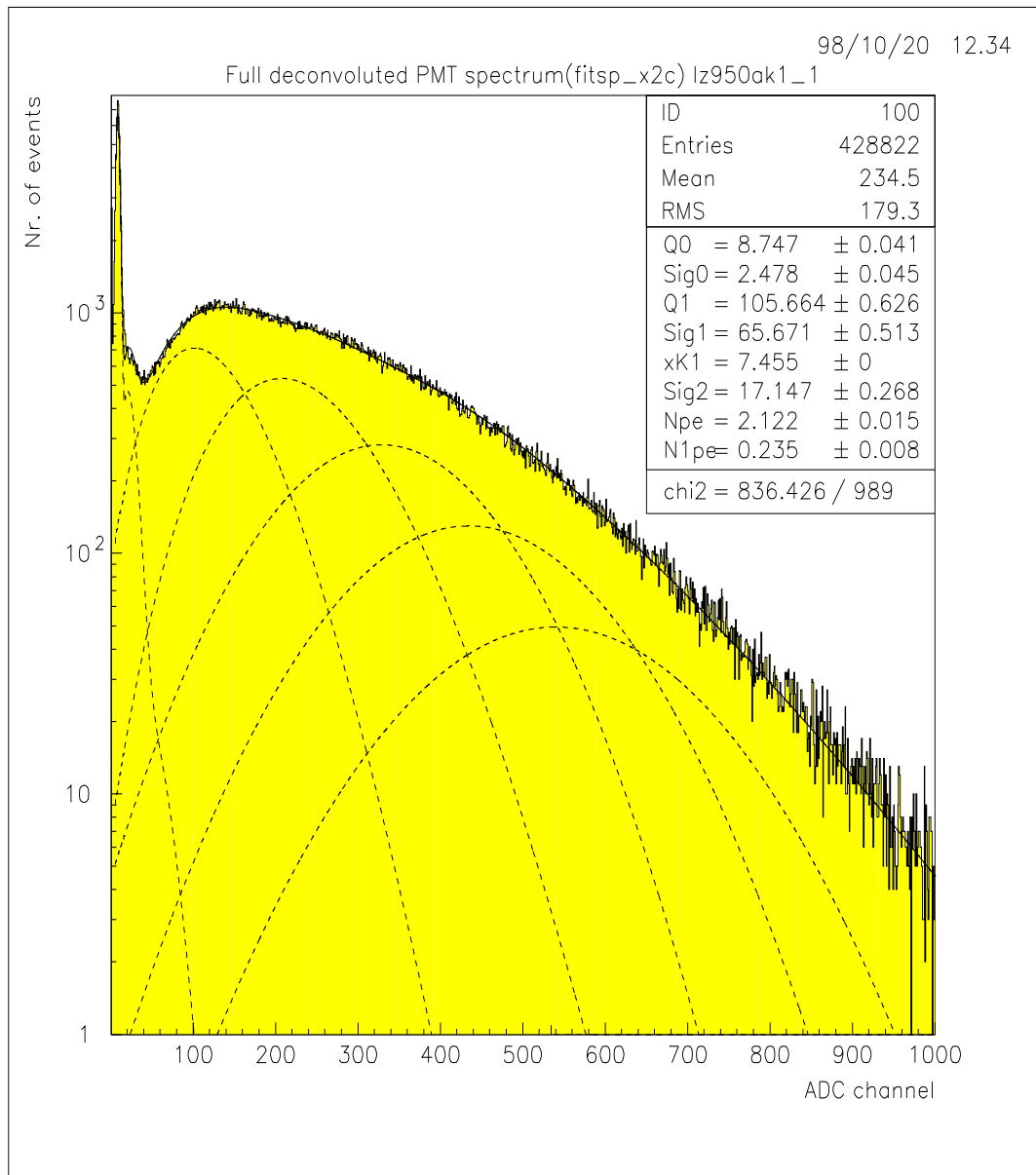


Figure 6: A typical deconvoluted *LED* spectrum taken by the PMT Hamamatsu *R5900* at *925 V*.

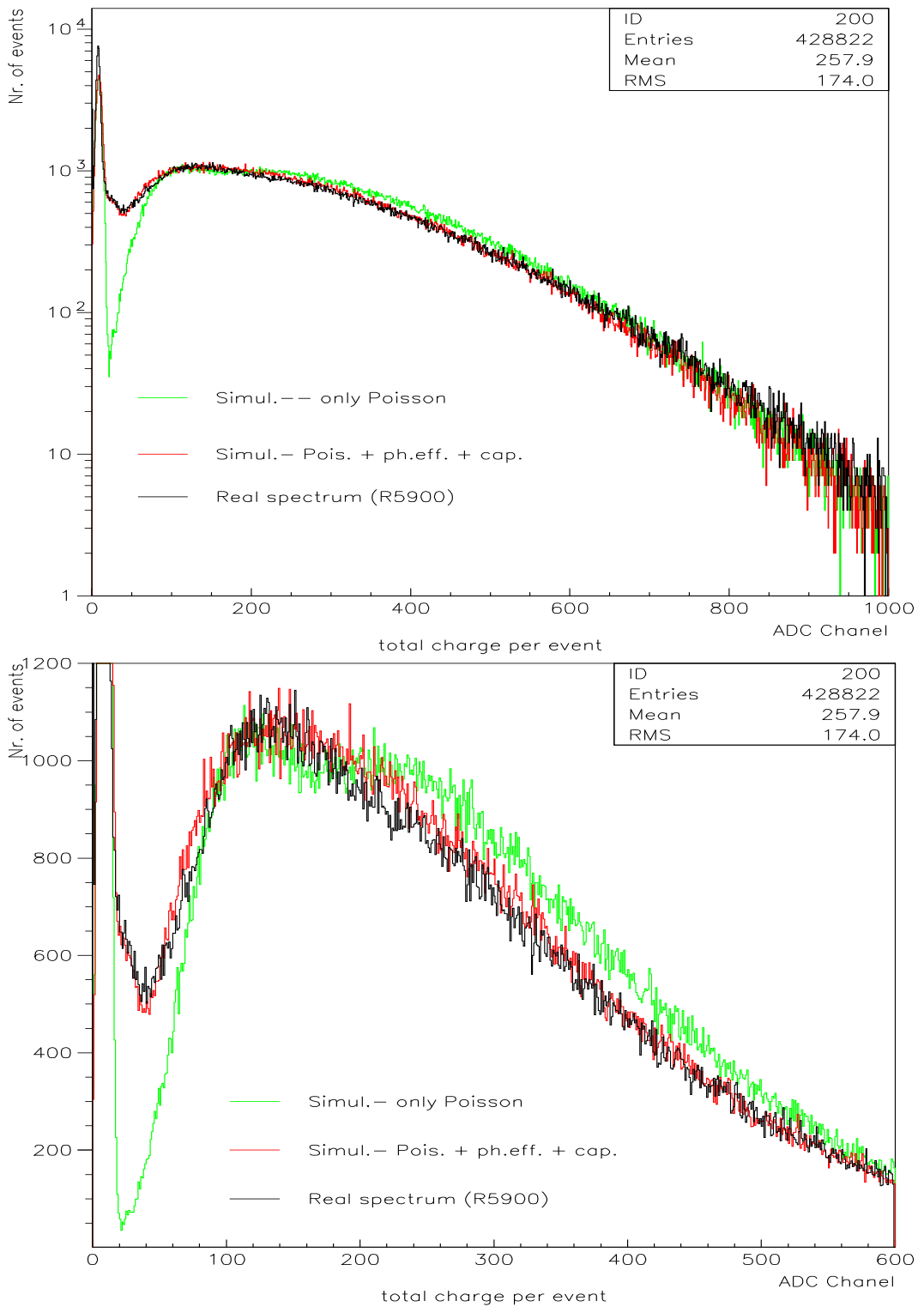


Figure 7: Comparison of the real spectrum taken at 925V by R5900 PMT (black line) with two simulation spectra: a) the ideal one (green line) - the multiplication process obeys Poisson law only, b) the case of spectrum with the additional processes involved ( the first dynode effect and dynode inhomogeneity of 25% ).

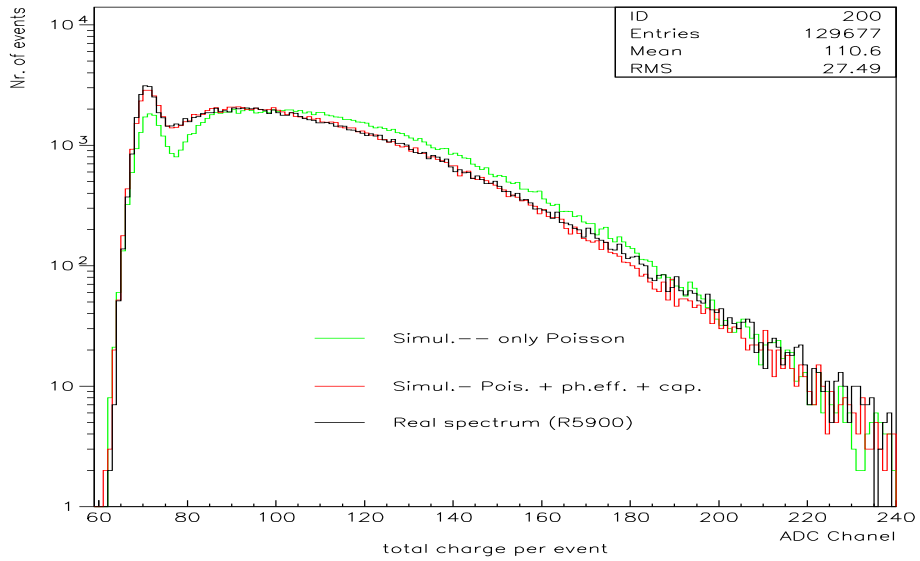


Figure 8: Comparison of the real spectrum taken at  $700\text{ V}$  by R5900 PMT (black line) with two simulation spectra: a) the ideal one (green line) - the multiplication process obeys Poisson law only, b) the case of spectrum with the additional processes involved ( the first dynode effect and dynode inhomogeneity of  $25\%$ ).

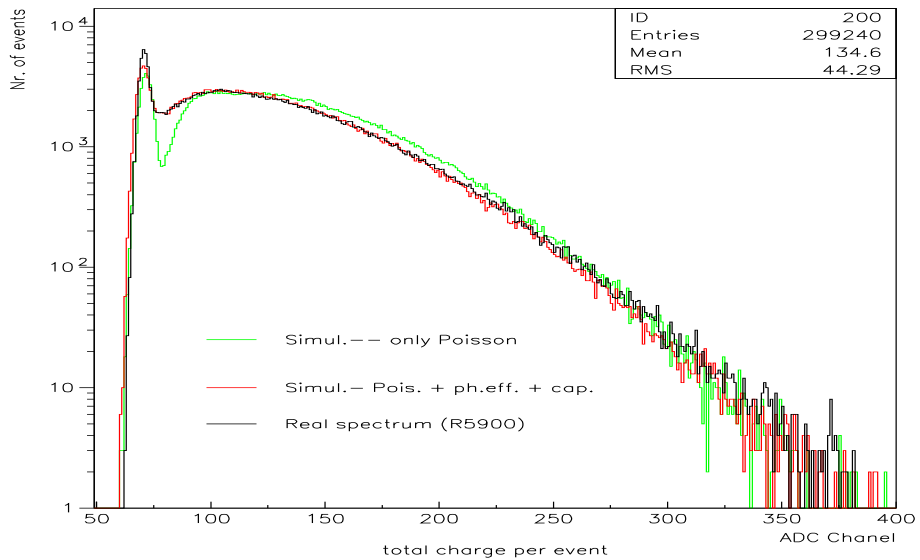


Figure 9: Comparison of the real spectrum taken at  $750\text{ V}$  by R5900 PMT (black line) with two simulation spectra: a) the ideal one (green line) - the multiplication process obeys Poisson law only, b) the case of spectrum with the additional processes involved ( the first dynode effect and dynode inhomogeneity of  $25\%$ ).



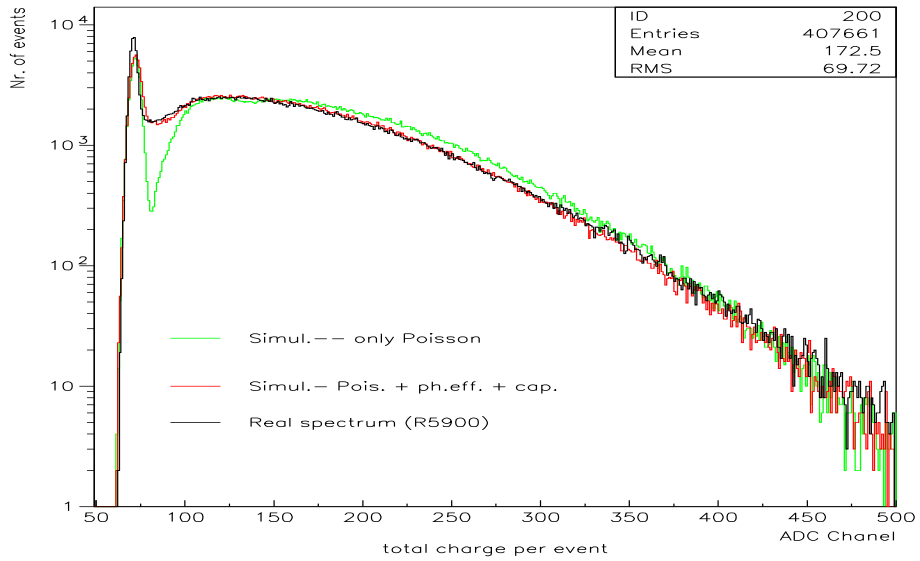


Figure 10: Comparison of the real spectrum taken at  $800\text{ V}$  by R5900 PMT (black line) with two simulation spectra: a) the ideal one (green line) - the multiplication process obeys Poisson law only, b) the case of spectrum with the additional processes involved ( the first dynode effect and dynode inhomogeneity of  $25\%$ ).

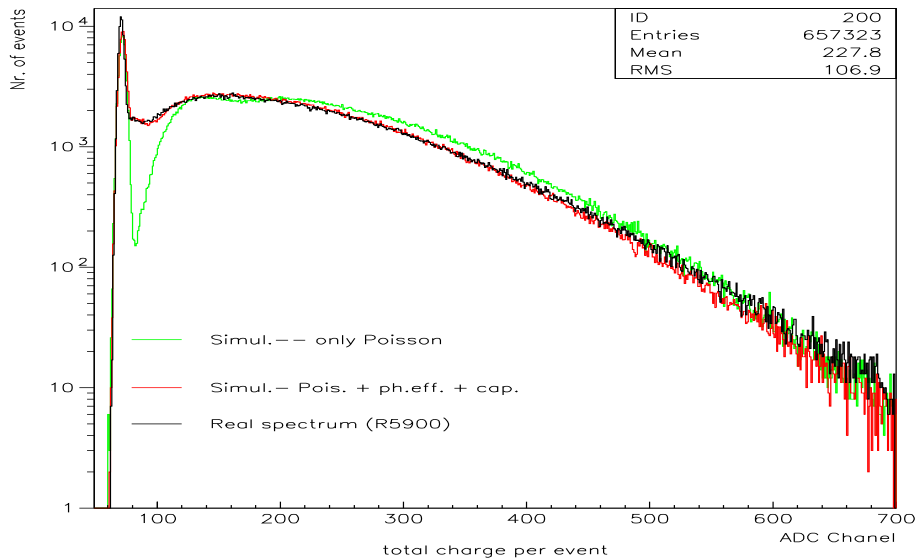


Figure 11: Comparison of the real spectrum taken at  $850\text{ V}$  by R5900 PMT (black line) with two simulation spectra: a) the ideal one (green line) - the multiplication process obeys Poisson law only, b) the case of spectrum with the additional processes involved ( the first dynode effect and dynode inhomogeneity of  $25\%$ ).